

Energetics and dissociative photodetachment dynamics of superoxide–water clusters: $\text{O}_2^-(\text{H}_2\text{O})_n$, $n=1-6$

A. K. Luong, T. G. Clements, M. Sowa Resat,^{a)} and R. E. Continetti

Department of Chemistry and Biochemistry, University of California, San Diego, 9500 Gilman Drive, La Jolla, California 92093-0314

(Received 20 October 2000; accepted 29 November 2000)

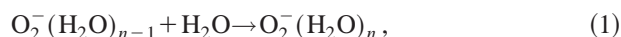
The dissociative photodetachment of $\text{O}_2^-(\text{H}_2\text{O})_{n=1-6}$ was studied at 388 and 258 nm using photoelectron–multiple-photofragment coincidence spectroscopy. Photoelectron spectra for the series indicate a significant change in the energetics of sequential solvation beyond the fourth water of hydration. Photoelectron–photofragment kinetic energy correlation spectra were also obtained for $\text{O}_2^-(\text{H}_2\text{O})_{1-2}$, permitting a determination of the first and second energies of hydration for O_2^- to be 0.85 ± 0.05 and 0.70 ± 0.05 eV, respectively. The correlation spectra show that the peak photofragment kinetic energy release in the dissociative photodetachment of $\text{O}_2^-(\text{H}_2\text{O})$ and $\text{O}_2^-(\text{H}_2\text{O})_2$ are 0.12 and 0.25 eV, respectively, independent of the photon and photoelectron kinetic energies. The molecular frame differential cross section for the three-body dissociative photodetachment: $\text{O}_2^-(\text{H}_2\text{O})_2 + h\nu \rightarrow \text{O}_2 + 2\text{H}_2\text{O} + e^-$ is also reported. The observed partitioning of momentum is consistent with either a sequential dissociation or dissociation from a range of initial geometries. © 2001 American Institute of Physics. [DOI: 10.1063/1.1342221]

I. INTRODUCTION

Many important chemical reactions occur in solution, yet detailed information regarding the molecular level interactions between the solvent and solute remain difficult to obtain. Despite the difficulty in characterizing the many-body interactions in solution, important steps in this direction have been taken using a variety of time-resolved spectroscopic techniques.^{1–3} Another approach to understanding condensed phase phenomena is by the stepwise increase in solvent number densities, a technique taken in a large number of studies of the energetics and dynamics of gas-phase clusters.^{4–8} Recently there have also been considerable advances in the infrared spectroscopy of small clusters, providing more direct information on the structures of these species.^{9–11} These studies of homogenous and heterogeneous clusters have provided direct insights into the effects of solvent–solvent and solute–solvent interactions on solvation dynamics and reveal information about the evolving energetics and geometries as cluster sizes increase, providing a link between our understanding of gas and condensed phase reaction dynamics. Superoxide–water clusters are the subject of the current study and represent an important prototypical system involving strong ion–dipole interactions. In the experiments reported here, negative-ion photodetachment spectroscopy is combined with the photoelectron–multiple-photofragment coincidence technique to obtain information on the energetics of sequential solvation of O_2^- by up to six waters and on the dissociative photodetachment (DPD) dynamics of $\text{O}_2^-(\text{H}_2\text{O})$ and $\text{O}_2^-(\text{H}_2\text{O})_2$.

There have been a number of studies of the $\text{O}_2^-(\text{H}_2\text{O})_n$ cluster ions. The earliest work by Kebarle and co-workers used high pressure mass spectrometry to study the heats of

formation of hydrated O_2^- clusters. By measuring the equilibrium constants, $K_{n-1,n}$, for the forward and reverse reactions for



Arshadi *et al.* determined the $\Delta H_{n-1,n}^0$ at 298 K for up to $n=3$ (0.80, 0.75, and 0.67 eV for $n=1, 2,$ and $3,$ respectively).¹² Yamdagni *et al.* later extended these studies to determine the temperature and solvent dependence of the equilibrium constants.¹³ More recent high pressure mass spectrometry experiments by Castleman and co-workers sought to understand how the reactions between O_2^- , CH_3CN , and SO_2 change as a function of an increasing number of water solvent molecules.^{4,5}

Further studies of the interactions between O_2^- and H_2O solvent molecules were carried out using photoelectron and photofragment translational spectroscopy to examine the energetics and dissociation branching ratios of $\text{O}_2^-(\text{H}_2\text{O})_n$ clusters. Johnson and co-workers used collision-induced dissociation, photodetachment, and photodissociation to probe the dependence of the photodissociation of O_2^- on cluster size.^{7,14} Buntine *et al.* studied the dissociation pathways that occur in the photodestruction of $\text{O}_2^-(\text{H}_2\text{O})$ in the 200–300 nm regime.¹⁴ These studies showed that while O_2^- remains intact in the water cluster, vibrational structure in the photoelectron spectrum was lost. In photodissociation experiments at 266 nm, (0.57 eV above the O_2^- photodissociation threshold) ionic products were observed that could not be explained without invoking a geminate recombination process involving the dissociated O atom and a hot $\text{O}(\text{H}_2\text{O})$ intermediate. Experiments by Lavrich *et al.* addressed the issue of whether the anion is bound on the surface of the cluster or internally by studying the excess energy dependence of the photodissociation probability for O_2^- in the cluster.⁷

Previously in our laboratory, Sherwood *et al.* used pho-

^{a)}Permanent address: Environmental Molecular Science Laboratory, P.O. Box 999, K8.88, Richland, WA 99352.

tofragment translational spectroscopy to study the dynamics of the dissociative photodetachment (DPD) in the superoxide–water cluster, which was confirmed to be the predominant channel for photodestruction at 524, 349, and 262 nm.¹⁵ These experiments were consistent with the previous measurements of Buntine *et al.*, which indicated a branching ratio of less than 5% ionic photodissociation versus photodetachment. The experiments by Sherwood *et al.* also showed that the photofragment translational energy release distribution is independent of the photon energy and peaks at a low value ~ 0.10 eV, suggesting that transfer of the significant vibrational excitation induced in the O₂ molecule upon photodetachment to the reaction coordinate in the neutral complex is highly inefficient. It was further concluded that the DPD of O₂⁻(H₂O) can be characterized as a Franck/Condon excitation to a weakly repulsive neutral potential energy surface.

The most recent work on these cluster systems by Weber *et al.* using Ar-nanomatrix-isolation infrared spectroscopy demonstrated that four H₂O molecules comprise the first solvation shell around O₂⁻.¹⁰ They observed a significant change in the IR spectra from broad unstructured features for the smaller superoxide hydrates to well-defined peaks for O₂⁻(H₂O)₄. Weber *et al.* reasoned that the sudden shift is due to the increased structural stability in the tetrahydrate when the first solvation shell is filled. In the smaller clusters, it was suggested that multiple conformers arising from the different possible arrangements of the H₂O molecule(s) around O₂⁻ lead to broadened features in the IR spectra.

Theoretically, the O₂⁻(H₂O)_{*n*} clusters have been the subject of several *ab initio* studies. At lower levels of theory, an asymmetric singly hydrogen bonded structure for O₂⁻(H₂O) was determined to be the most stable species.^{16,17} However, using UMP2 calculations with larger basis sets, Lee *et al.* found the doubly hydrogen-bonded C_{2_v} structure to have the minimum energy, although the difference in energy was very small.¹⁸ There has been much less work on the larger superoxide–water clusters. In a study by Curtiss *et al.*, the stabilities of the singly- and doubly-hydrogen-bonded structures of O₂⁻(H₂O)_{2,4} were determined to be very similar.¹⁶ The general conclusion drawn from these theoretical calculations is that the potential energy surfaces for these small superoxide–water clusters are relatively flat, with a number of local minima.

In the experiments reported here, photoelectron–photofragment coincidence (PPC) spectroscopy is used to examine photodetachment and DPD of the superoxide–water clusters. These experiments use fast ion beam photodetachment techniques and high-efficiency photoelectron and multiple-photofragment detectors to measure the photoelectron and photofragments from a single DPD event in coincidence. The time- and position-sensitive detectors provide detailed information about the energy and angular distributions of the photofragments resulting from photodetachment of an anion precursor, allowing insights into the energetics, dissociation dynamics, and possible structures of the neutral cluster. In particular, the experiments on the O₂⁻(H₂O)_{*n*} clusters presented here seek to further characterize the energetics of solvation for up to six water molecules, and extend our pre-

vious study of the DPD of O₂⁻(H₂O) to include PPC measurements and to provide the first experimental insights into the three-body DPD process of O₂⁻(H₂O)₂. In the next sections, a brief description of the experimental method is presented, followed by results for the dissociative photodetachment of superoxide–water cluster anions.

II. EXPERIMENT

In these experiments, PPC spectroscopy is applied to study the dissociation dynamics of transient neutral species by photodetachment of a mass-selected anion precursor. The energy of the neutral is determined by measurement of the photoelectron kinetic energy. The photofragments resulting from any subsequent dissociation of the neutral complex are detected using a multiparticle detector, yielding the kinetic energies and recoil angles of all the particles produced in an individual event. The experimental apparatus has been described in detail in a previous publication,¹⁹ and is briefly reviewed here.

The anion precursors were generated using a pulsed supersonic expansion of pure O₂ passed over room temperature H₂O intersected by a 1 keV electron beam. The anions passed through a skimmer were accelerated to 4 keV, mass selected by time-of-flight, and electrostatically guided into the interaction region. Any neutrals generated before the interaction region were removed from the ion beam in the time-of-flight region by use of a set of vertical deflectors and a neutral beam blocker. A focused linearly polarized laser beam of the second (388 nm) or third (258 nm) harmonic of a pulsed Ti:sapphire fundamental [1.2 ps full width at half maximum (FWHM)] then crossed the ion beam at 90°. Photoelectrons were detected using one of two opposed time- and position-sensitive photoelectron detectors, perpendicular to the ion and laser beam paths. The measured laboratory kinetic energies of the photoelectrons were corrected for the Doppler shift from the fast ion beam yielding the center-of-mass (CM) electron kinetic energy (*e*KE), with a resolution $\Delta E/E \sim 5\%$ at 1.3 eV. Measurement of the electron energy defines the internal energy of the transient neutral species produced by photodetachment. If this neutral species dissociates, the resulting photofragments are detected in coincidence by a multiparticle time- and position-sensitive detector located 104 cm downstream of the interaction region. Residual ions leaving the laser interaction region are electrostatically deflected out of the beam into an ion detector. The multiparticle detector consists of four quadrants, each of which is a crossed-delay-line anode detector with the capability to detect the *x,y* positions and time-of-arrival of any two photofragments that are at least 10 ns apart. This configuration permits the apparatus to directly record the number of photofragments generated in the dissociation process, and to measure in coincidence the time and position of impact of all the particles. By conservation of linear momentum, the photofragment masses and the CM kinetic energy and recoil angles of all the photofragments are determined for each event. The CM kinetic energy of each photofragment is then summed to yield the total photofragment trans-

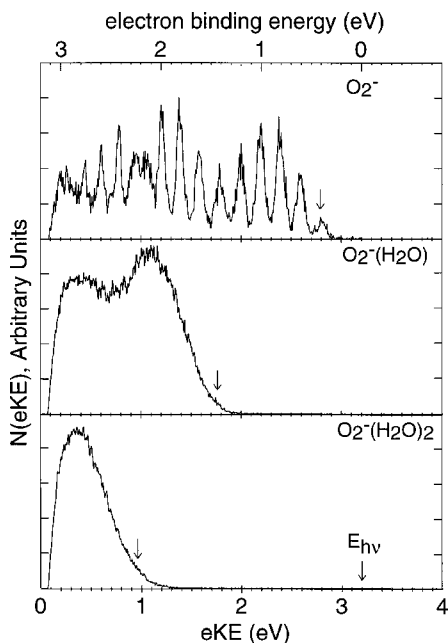


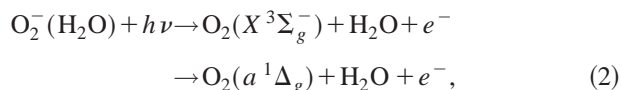
FIG. 1. The photoelectron spectra for $O_2^-(H_2O)_n$ for $n=0-2$ at 388 nm, where the arrows indicate the approximate ADEs.

lational energy release (E_T) spectrum, giving $\Delta E/E \sim 15\%$ at 0.7 eV.

III. RESULTS

A. Photoelectron spectra

The photoelectron spectra for $O_2^-(H_2O)_n$ for $n=0-2$ at 388 nm are shown in Fig. 1. As previously demonstrated by Johnson and co-workers for $O_2^-(H_2O)$, the vibrational structure present in the well-known photoelectron spectrum of bare O_2^- is absent for $O_2^-(H_2O)_n$ clusters.¹⁴ However, for $O_2^-(H_2O)$, two broad peaks at $eKE=1.1$ and 0.4 eV are distinguishable but shifted by ~ 1.0 eV lower compared to O_2^- . These features are consistent with dissociative photodetachment to the ground and first excited electronic states of O_2 :



in agreement with previous work by Buntine *et al.* at 355 nm.¹⁴ For the $n=2$ anion, the photoelectron spectrum is shifted to even lower eKE by ~ 0.8 eV relative to the singly hydrated O_2^- , and only the peak for the ground electronic state is observable.

To study the larger superoxide-water clusters, photoelectron spectra of $O_2^-(H_2O)_n$ for $n=1-6$ were measured at 258 nm as shown in Fig. 2. At this wavelength, photodetachment of $O_2^-(H_2O)$ to $O_2(b^1\Sigma_g^+) + H_2O + e^-$ also becomes accessible. The sharp peak near 0 eV present in the spectra at this wavelength arises from electrons produced by the scattering of the laser off surfaces in the spectrometer. The form of this background was measured in a separate experiment and is shown as the dotted line curve. As the number of water molecules increases from one to six, the features in the photoelectron spectra shift towards lower eKE , illustrating

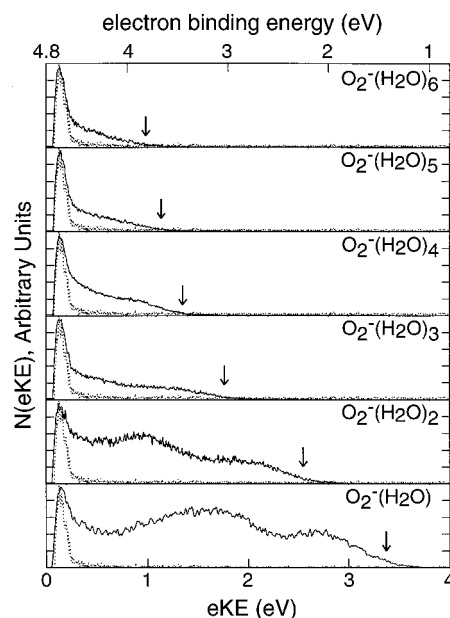


FIG. 2. The photoelectron spectra for $O_2^-(H_2O)_n$, $n=1-6$ at 258 nm are shown as solid lines, with the ADEs discussed in the text indicated by the arrows. The dotted curves show the form of the laser-related photoelectron background. In all cases at low eKE there is expected to be real signal, so the background curves are an overestimation of the actual background.

the increase in the adiabatic detachment energy (ADE) of the excess electron in the $O_2^-(H_2O)_n$ clusters. As discussed below, the photoelectron and photofragment kinetic energy correlation spectra for $O_2^-(H_2O)_{n=1-2}$ can be used to obtain values for the ADE for the singly and doubly hydrated cluster systems. These values are indicated with arrows in Figs. 1 and 2. By analogy to the two smaller clusters, arrows showing the approximate ADE for $O_2^-(H_2O)_{n=3-6}$ are also shown in Fig. 2. It is interesting to note that the incremental decrease in the ADE between sequentially larger clusters is significantly smaller for $n=4-6$, as shown in Table I and further discussed below.

B. Photoelectron-photofragment correlation spectra

The coincident measurement of the photoelectron and photofragments for each event allows acquisition of the photoelectron-photofragment translational energy correlation spectrum, $N(E_T, eKE)$. When clusters undergo DPD, this measurement provides a complete kinematic description of the process by revealing the kinetic energy carried away by the photoelectron and the dissociating photofragments in coincidence. The $N(E_T, eKE)$ spectra for $O_2^-(H_2O)_n$, $n=1,2$ at 388 nm are shown in Fig. 3. These spectra are two-dimensional histograms of the correlated events, with eKE along the y -axis, and E_T along the x -axis. Hence, the contour features represent the distribution of events exhibiting a particular partitioning of E_T and eKE among the products. Given that the rate of false coincidences for detecting one photoelectron and three photofragments is $\sim 4\%$,¹⁹ a diagonal line drawn at the 6% contour gives a conservative indication of the maximum kinetic energy (KE_{max}) for DPD. This line provides a direct determination of the stability of $O_2^-(H_2O)_n$ relative to $O_2 + nH_2O + e^-$, (the DPD threshold),

TABLE I. Summary of energetics in eV for $O_2^-(H_2O)_n$, $n=0-6$ clusters.

	ADE ^a	$\Delta ADE_{n-1,n}$	VDE	$\Delta VDE_{n-1,n}$	VDE-ADE	DPD Threshold
O_2^-	0.45 ^{b,c}		0.82		0.37	
$O_2^-(H_2O)$	1.42	0.97	2.03	1.21	0.61	1.30
$O_2^-(H_2O)_2$	2.25	0.83	2.77	0.74	0.52	2.00
$O_2^-(H_2O)_3$	3.03	0.78		
$O_2^-(H_2O)_4$	3.45	0.42		
$O_2^-(H_2O)_5$	3.67	0.22		
$O_2^-(H_2O)_6$	3.77	0.10		

^aUncertainties in the ADE, VDE, and DPD threshold values are estimated to be ± 0.05 eV.

^bThe ADE for O_2^- is equal to the adiabatic electron affinity.

^cReference 20.

^dVDEs were not tabulated for $n=3-6$ since the peak positions were not assignable.

if it is assumed that some of the products are produced in their vibrational and rotational ground states and that the parent anions are internally cold. Since the cluster anions are produced in a pulsed supersonic expansion, they are expected to be vibrationally cold: the O_2^- photoelectron spectrum shown in Fig. 1 shows no hot bands. However, low frequency modes in the clusters are likely to exhibit some vibrational excitation. Thus, some events may be expected to occur above the KE_{max} line drawn at 1.90 eV in the left frame of Fig. 3.

Energetic considerations indicate that the only channel accessed in the DPD process is the production of $O_2 + nH_2O + e^-$. The photon energy of 3.20 eV at 388 nm indicates that $O_2^-(H_2O)$ is stable by 1.30 eV relative to the products. Given the electron affinity of O_2^- of 0.45 eV,²⁰ this yields the dissociation energy for $O_2^-(H_2O) \rightarrow O_2^- + H_2O$, $\Delta D_0 = 0.85 \pm 0.05$ eV. The stated error accounts for the energy resolution in the photoelectron and photofragment detectors. Likewise, an analogous diagonal line at 1.20 eV can be drawn in the right frame for the $N(E_T, eKE)$ of $O_2^-(H_2O)_2$. Consideration of the energetics indicates that $O_2^-(H_2O)_2$ is 2.00 eV more stable than $O_2 + 2H_2O + e^-$, or that $\Delta D_0 = 0.70 \pm 0.05$ eV for the process $O_2^-(H_2O)_2 \rightarrow O_2^-(H_2O) + H_2O$. In the absence of parent anion vibrational excitation, which is expected to be small in the pulsed molecular beam ion source, these results represent upper limits to the true bond dissociation energy since the assumption is made that some products are produced with no internal excitation.

At 258 nm, the $N(E_T, eKE)$ spectra for $O_2^-(H_2O)_{1,2}$ are shown in Fig. 4. The correlation spectra are essentially identical to those obtained at 388 nm, except for the shift in energy along the eKE axis due to the difference in photon energy. At both wavelengths, the E_T distribution of the singly hydrated O_2^- cluster peaks at ~ 0.12 eV, while the doubly hydrated cluster peaks at ~ 0.25 eV. It is also observed for both clusters that there is not a significant correlation between E_T and eKE at the two wavelengths, except for the conservation of energy. The ADEs for $O_2^-(H_2O)$ and $O_2^-(H_2O)_2$, discussed above, were estimated in light of this by subtracting the peak E_T from the DPD threshold determined from the KE_{max} limits in the correlation spectra for each cluster. These results confirm that the E_T distributions are independent of the initial available energy from the photon, consistent with Franck-Condon photodetachment to a repulsive region of the neutral surface.¹⁵

C. Molecular-frame differential cross section

Additional insights into the three-body dissociation of the $O_2(H_2O)_2$ cluster that occurs after photodetachment may be obtained by analysis of the relative angular distributions of the fragments. One way to do this is by examination of the molecular-frame differential cross section (MF-DCS) in momentum space. The MF-DCS is a contour map in which the CM momentum distribution of the lightest particle lies along the positive x -axis, while the momentum vector distributions for the other two fragments appear above and below the

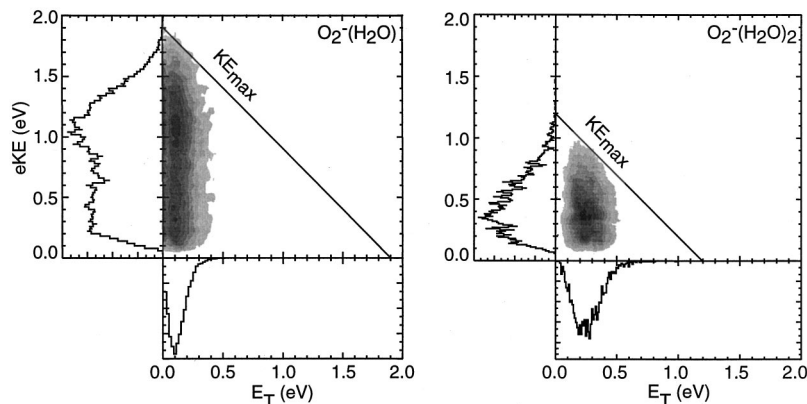


FIG. 3. The $N(E_T, eKE)$ spectra for the $O_2^-(H_2O)_n$ for $n=1$ and 2 at 388 nm. KE_{max} marks the DPD threshold for these two systems as discussed in the text.

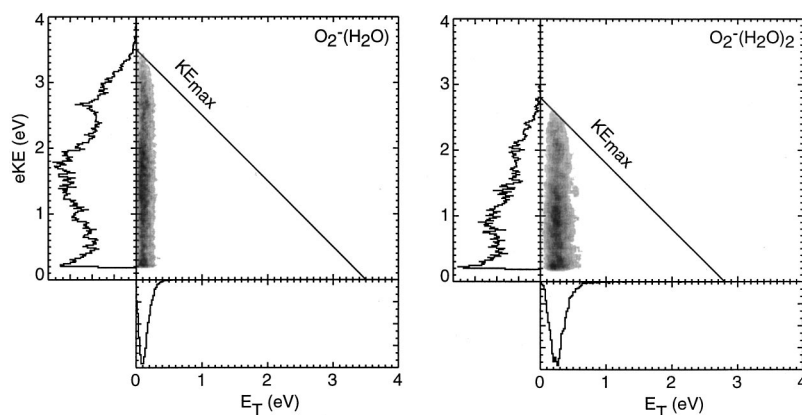


FIG. 4. The $N(E_T, eKE)$ spectra for $O_2^-(H_2O)_n$ for $n = 1$ and 2 at 258 nm. KE_{max} marks the DPD threshold for these two systems at this wavelength as discussed in the text.

x -axis. This spectrum provides insights into both the momentum and relative angular distributions resulting from the DPD process. If dissociation is rapid relative to the rotational period of the neutral complex, the centroids of the anisotropic momentum vector distributions in the MF-DCS directly map the instantaneous recoil directions of the photo-fragments. Thus, this method can provide valuable insights into the structure of the species at the time of dissociation.²¹ However, if the dissociation is slow relative to the rotational period of the transient neutral, the MF-DCS will show relatively wide momentum vector distributions for the photo-fragments and structural inferences are limited. Another factor inhibiting an unambiguous interpretation of the MF-DCS spectra is the presence of multiple conformers leading to the same dissociation channels.

Figure 5 shows the MF-DCS for the DPD process $O_2^-(H_2O)_2 + h\nu \rightarrow O_2 + 2H_2O + e^-$ at 388 and 258 nm in the top and bottom frames, respectively. The one-dimensional distribution curve along the x -axis shows the direction and peak value of the momentum of the fast H_2O product used as the reference particle. The MF-DCS indicates that the fast H_2O product carries away the largest momentum, with the balance shared between O_2 and the slow H_2O product. The O_2 and slow H_2O product momenta are distributed over a wide range of recoil angles relative to the fast H_2O product. The O_2 distribution exhibits a sharp peak at low momentum with a decreasing distribution towards larger momenta, similar to the slow H_2O product. Both the O_2 and H_2O distributions show evidence for some bimodality in the distribution, i.e., a peak or plateau at larger momenta.

IV. DISCUSSION

The results reported here provide information on the energetics of the solvation of O_2^- by water and the dissociation dynamics of the energized neutral clusters produced by photodetachment. A number of energetic quantities are determined in these experiments from the observed photoelectron and photoelectron-photofragment correlation spectra. These include thresholds for DPD of $O_2^-(H_2O)$ and $O_2^-(H_2O)_2$, from which the ADE for these systems as well as the dissociation energies of the anions are determined. Based on the results for the $n=1$ and 2 clusters, the ADEs for the $n=3-6$ clusters were estimated from the photoelectron spectra. The observed increase in ADE with addition of H_2O

shown in the photoelectron spectra in Fig. 2 and tabulated in Table I has been previously observed for other anions solvated by water.²² The large shift of the features in the PES of $O_2^-(H_2O)$ relative to O_2^- is dominated by stabilization of the anion by strong ion-dipole interactions in the cluster. As the number of solvating water molecules goes from zero to six, there is an increase in the solvation energy (and the ADE). As more waters are added, the incremental increase in the ADE decreases, in accord with high pressure mass spectrometry experiments on $O_2^-(H_2O)_{0-3}$ by Arshadi *et al.*¹² As the results in Table 1 show, the difference in ADE from $n=2$ to $n=3$ drops only slightly from $n=1$ to $n=2$. It is interesting to note that addition of a fifth water to $O_2^-(H_2O)_4$ only increases the ADE by 0.22 eV, a value which drops by more

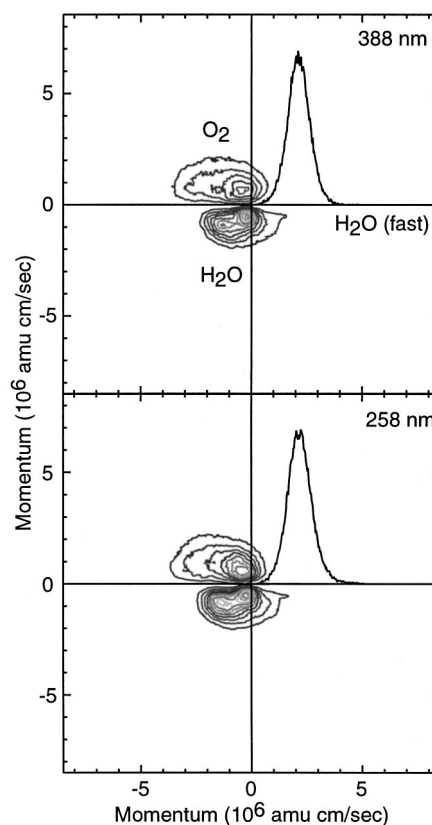


FIG. 5. MF-DCS spectra of $O_2^-(H_2O)_2$ at 258 and 388 nm. The reference particle for these spectra is the fast H_2O product.

than a factor of two as a sixth water is added. These incremental changes in the ADE of less than 0.25 eV as additional water molecules are added to the $\text{O}_2^-(\text{H}_2\text{O})_4$ cluster are consistent with the spectroscopic observations by Weber *et al.* that showed a significant sharpening of the features in the IR spectrum of $\text{O}_2^-(\text{H}_2\text{O})_4$ assigned to completion of the first solvation shell.¹⁰

One of the most striking features of the $\text{O}_2^-(\text{H}_2\text{O})_n$ photoelectron spectra is the loss of the considerable vibrational structure observed in photodetachment of the molecular anions. The $N(E_T, e\text{KE})$ spectra discussed below show that this loss of vibrational structure is probably not the result of lifetime broadening as previously seen to be the case in photodetachment of oxygen dimer anion, O_4^- .²³ In the case of O_4^- , photodetachment produced neutral O_4 with 0.4 eV repulsive energy, followed by a rapid, vibrationally adiabatic dissociation process to O_2 products. As discussed by Sherwood *et al.*, the relatively long distance (2.8 Å) calculated between O_2^- and H_2O is not expected to lead to significant repulsion on the neutral surface.^{15,18} In the case of the $\text{O}_2^-(\text{H}_2\text{O})_n$ clusters it is likely that broadening primarily arises from spectral congestion due to a broad range of initial geometries with slightly different ADEs. A detailed analysis of the photoelectron spectra of the $\text{O}_2^-(\text{H}_2\text{O})_n$ for structural properties is beyond the scope of this work, but it is interesting to examine the trends in the vertical detachment energies (VDEs) for $\text{O}_2^-(\text{H}_2\text{O})_{1,2}$ relative to free O_2^- as shown in Table 1. Changes in the Franck–Condon distribution for photodetachment are expected to appear in the difference between the ADE and the VDE. As noted in Table 1, this difference is considerably larger for $\text{O}_2^-(\text{H}_2\text{O})$ and $\text{O}_2^-(\text{H}_2\text{O})_2$ than it is for O_2^- . This implies that photodetachment of these clusters is producing excitation in degrees of freedom other than the vibrational and electronic states of O_2 due to interactions with the solvating water molecules.

In addition to the photoelectron spectra, the present experimental results yield the $N(E_T, e\text{KE})$ correlation spectra of $\text{O}_2^-(\text{H}_2\text{O})_{1,2}$ at 388 and 258 nm, showing how energy is partitioned in the DPD of $\text{O}_2^-(\text{H}_2\text{O}) + h\nu \rightarrow \text{O}_2 + \text{H}_2\text{O} + e^-$, and the three-body DPD of $\text{O}_2^-(\text{H}_2\text{O})_2 + h\nu \rightarrow \text{O}_2 + 2\text{H}_2\text{O} + e^-$. The observation that $e\text{KE}$ and E_T are uncorrelated, beyond the conservation of energy, and the independence of the E_T distribution on the photon wavelength illustrates that there is little coupling between the internal energy, in particular the vibration or electronic state of the nascent O_2 , and the dissociation coordinate. Furthermore, the structureless E_T distribution peaks at only 0.12 eV for dissociation of $\text{O}_2^-(\text{H}_2\text{O})$, consistent with photodetachment to a weakly repulsive region of the neutral potential energy surface, confirming earlier results obtained in this laboratory and by theoretical predictions.^{15,18} These results indicate that dissociation of excited $\text{O}_2^-(\text{H}_2\text{O})$ complexes produced by photodetachment is likely to be both vibrationally and electronically adiabatic.

The addition of another water molecule to the cluster to form $\text{O}_2^-(\text{H}_2\text{O})_2$ results in doubling of the peak E_T to 0.25 eV in the three-body DPD. The increase in E_T with the additional water molecule appears nonintuitive since it might be expected that some of the energy released in the dissocia-

tion would be transferred into the now-increased number of internal degrees of freedom in the system. However, if the Franck–Condon overlap with the neutral surface for $\text{O}_2^-(\text{H}_2\text{O})_2$ leaves the nascent neutral $\text{O}_2(\text{H}_2\text{O})_2$ in a geometry where each water experiences a repulsion similar to that in $\text{O}_2(\text{H}_2\text{O})$, this doubling of the kinetic energy release is not surprising. Alternatively, it is possible that owing to the structure of the nascent $\text{O}_2(\text{H}_2\text{O})_2$ complex, transfer of internal energy (vibration of the O_2 molecule) may be more facile than in the singly hydrated $\text{O}_2(\text{H}_2\text{O})$. It is interesting to note in this regard that the vibrational quantum of O_2 is approximately 0.2 eV, suggesting that transfer of one vibrational quantum to translation in the $\text{O}_2(\text{H}_2\text{O})_2$ cluster could explain the observed difference in E_T in the two systems.

The three-body DPD dynamics for $\text{O}_2^-(\text{H}_2\text{O})_2$ are revealed in the MF-DCSs shown in Fig. 5. The MF-DCSs at both wavelengths are similar, and show that the fast water carries away a relatively narrow range of momenta while the slow H_2O and O_2 products have a broader momentum distribution and a broad angular distribution relative to the center-of-mass of the system. The broad distribution in momenta for the slow H_2O and O_2 products suggests that this dissociation may be sequential, with the two H_2O products leaving the O_2 at different times. It is also possible that the multiple conformers of $\text{O}_2^-(\text{H}_2\text{O})$ that lead to the broadened photoelectron spectra also lead to broadening in the MF-DCS. A more detailed interpretation of the MF-DCS results will have to await further theoretical developments.

V. CONCLUSION

In these experiments, PPC spectroscopy was used to study the energetics and dissociation dynamics of $\text{O}_2^-(\text{H}_2\text{O})_n$, $n = 1-6$ clusters. A marked decrease in the incremental change of the ADE as H_2O is added to the clusters suggests that the first solvation shell is comprised of four water molecules complexed to O_2^- , in agreement with the recent report by Weber *et al.*¹⁰ The first coincidence studies of the dissociative photodetachment dynamics of $\text{O}_2^-(\text{H}_2\text{O})$ and $\text{O}_2^-(\text{H}_2\text{O})_2$ were also carried out. The measured $N(E_T, e\text{KE})$ spectra show that the dominant decay channel produces $\text{O}_2 + n\text{H}_2\text{O} + e^-$, and the first and second hydration energies of O_2^- were found to be 0.85 and 0.70 ± 0.05 eV, respectively. The energy correlation spectra at 388 and 258 nm for both clusters show that the $N(e\text{KE})$ and $N(E_T)$ distributions are uncorrelated except for conservation of energy, which is attributable to an inefficient transfer of the nascent internal energy (vibrational and electronic) in the neutral O_2 to the dissociation coordinate of the complex. At 258 nm, the three lowest-lying states of O_2 , ${}^3\Sigma_g^-$, ${}^1\Delta_g$, ${}^1\Sigma_g^+$ are all produced in the DPD of $\text{O}_2^-(\text{H}_2\text{O})$, with no effect on the dissociation dynamics. Finally, the MF-DCS spectrum obtained for $\text{O}_2^-(\text{H}_2\text{O})_2$ suggests that either the dissociation is a sequential process, where the primary dissociation produces a fast H_2O product and a transient $\text{O}_2(\text{H}_2\text{O})$ cluster, or that the presence of multiple conformers of $\text{O}_2^-(\text{H}_2\text{O})_2$ lead to the observed broad momentum and angular distributions of the $\text{O}_2 + 2\text{H}_2\text{O}$ products. These observations should provide a

critical test of future high-level *ab initio* structure and dynamics calculations on these prototypical ion–dipole clusters.

ACKNOWLEDGMENTS

This work was supported by the Chemistry Division of the National Science Foundation under Grant CHE 97-00142. R.E.C. is a Camille Dreyfus Teacher–Scholar, an Alfred P. Sloan Research Fellow, and a Packard Fellow in Science and Engineering. A.K.L. received support from AFOSR-AASERT Grant F49620-97-1-0387, and T.G.C. received support from AFOSR Grant F49620-96-1-0220. Acquisition of the laser used in these studies was assisted by AFOSR DURIP Grant F49620-97-1-0255.

- ¹M. T. Zanni, B. J. Greenblatt, A. V. Davis, and D. M. Neumark, *J. Chem. Phys.* **111**, 2991 (1999).
²A. Sanov, T. Sanford, S. Nandi, and W. C. Lineberger, *J. Chem. Phys.* **111**, 664 (1999).
³A. Burroughs, T. Van Marter, and M. C. Heaven, *J. Chem. Phys.* **111**, 2478 (1999).
⁴X. Yang, X. Zhang, and A. W. Castleman, *J. Phys. Chem.* **95**, 8520 (1991).
⁵X. Yang and A. W. Castleman, *J. Phys. Chem.* **95**, 6182 (1991).
⁶L. Lehr, M. T. Zanni, C. Frischkorn, R. Weinkauff, and D. M. Neumark, *Science* **284**, 635 (1999).

- ⁷D. J. Lavrich, M. A. Buntine, D. Serxner, and M. A. Johnson, *J. Phys. Chem.* **99**, 8453 (1995).
⁸J.-H. Choi, K. T. Kuwata, B.-M. Haas, Y. Cao, M. S. Johnson, and M. Okumura, *J. Chem. Phys.* **100**, 7153 (1994).
⁹P. Ayotte, G. H. Weddle, C. G. Bailey, and M. A. Johnson, *J. Chem. Phys.* **110**, 6268 (1999).
¹⁰J. M. Weber, J. A. Kelley, S. B. Nielsen, P. Ayotte, and M. A. Johnson, *Science* **287**, 2461 (2000).
¹¹J. H. Choi, K. T. Kuwata, Y. B. Cao, and M. Okumura, *J. Phys. Chem. A* **102**, 503 (1998).
¹²M. Arshadi and P. Kebarle, *J. Phys. Chem.* **74**, 1483 (1970).
¹³R. Yamdagni, J. D. Payzant, and P. Kebarle, *Can. J. Chem.* **51**, 2507 (1973).
¹⁴M. A. Buntine, D. J. Lavrich, C. E. Dessent, M. G. Scarton, and M. A. Johnson, *Chem. Phys. Lett.* **216**, 471 (1993).
¹⁵C. R. Sherwood and R. E. Continetti, *Chem. Phys. Lett.* **258**, 171 (1996).
¹⁶L. A. Curtiss, C. A. Melendres, A. E. Reed, and F. Weinhold, *J. Comput. Chem.* **7**, 294 (1986).
¹⁷K. Ohta and K. Morokuma, *J. Phys. Chem.* **91**, 401 (1987).
¹⁸E. P. F. Lee and J. M. Dyke, *Mol. Phys.* **74**, 333 (1991).
¹⁹K. A. Hanold, A. K. Luong, T. G. Clements, and R. E. Continetti, *Rev. Sci. Instrum.* **70**, 2268 (1999).
²⁰M. J. Travers, D. C. Cowles, and G. B. Ellison, *Chem. Phys. Lett.* **164**, 449 (1989).
²¹A. K. Luong, T. G. Clements, and R. E. Continetti, *J. Phys. Chem. A* **103**, 10237 (1999).
²²R. G. Keesee and A. W. Castleman, in *Ion and Cluster Ion Spectroscopy and Structure*, edited by J. P. Maier (Elsevier, New York, 1989), p. 275.
²³K. A. Hanold and R. E. Continetti, *Chem. Phys.* **239**, 493 (1998).